Research Square

Preprints are preliminary reports that have not undergone peer review.
They should not be considered conclusive, used to inform clinical practice,
or referenced by the media as validated information.

TMOD3 drives malignant progression in pancreatic cancer through physical interaction with LRRFIP1

Chao Shen
The First Hospital of Jiaxing, The Affiliated Hospital of Jiaxing University
Xiaoyu Qian
The First Hospital of Jiaxing, The Affiliated Hospital of Jiaxing University
Liang Chen
The First Hospital of Jiaxing, The Affiliated Hospital of Jiaxing University
Jian Tang
The First Hospital of Jiaxing, The Affiliated Hospital of Jiaxing University
Liu Xu
xuliu34@126.com

The First Hospital of Jiaxing, The Affiliated Hospital of Jiaxing University

Research Article

Keywords: Pancreatic adenocarcinoma, TMOD3, LRRFIP1

Posted Date: November 5th, 2026

DOI: https://doi.org/10.21203/rs.3.rs-11440660/v1

License: This work is licensed under a Creative Commons Attribution 4.0 International License.
Read Full License

Additional Declarations: No competing interests reported.

Abstract

Pancreatic ductal adenocarcinoma (PDAC) is a highly lethal malignancy characterized by rapid progression and early metastasis. Although Tropomodulin 3 (TMOD3) regulates cytoskeletal dynamics, its clinical significance and molecular mechanisms in PDAC remain unclear. Here, we investigated the oncogenic role of TMOD3 in PDAC using the GEPIA database, a human tissue microarray, *in vitro* functional assays, and *in vivo* models of tumor growth and metastasis. We found that TMOD3 is significantly upregulated in PDAC tissues, correlating strongly with advanced tumor stage and poor overall survival. Functionally, TMOD3 knockdown markedly inhibited PDAC cell proliferation, migration, and invasion *in vitro*, and suppressed tumorigenicity and lung metastasis *in vivo*. Mechanistically, STRING prediction and endogenous co-immunoprecipitation revealed that TMOD3 physically interacts with Leucine-rich repeat flightless-interacting protein 1 (LRRFIP1) without altering its transcription. Furthermore, rescue experiments demonstrated that silencing LRRFIP1 effectively abrogated TMOD3-induced malignant phenotypes and tumor growth both *in vitro*and *in vivo*. Collectively, our findings demonstrate that the TMOD3/LRRFIP1 axis drives PDAC progression and metastasis, highlighting TMOD3 as a promising prognostic biomarker and therapeutic target.

Significance

The high lethality of pancreatic cancer urgently requires the identification of novel therapeutic targets. This study is the first to reveal that TMOD3 strongly drives tumor proliferation and metastasis by physically interacting with LRRFIP1. Elucidating this novel TMOD3/LRRFIP1 oncogenic axis provides a promising prognostic biomarker and a compelling rationale for targeted interventions.

Introduction

Pancreatic ductal adenocarcinoma (PDAC) is among the most aggressive and lethal malignancies worldwide, projected to become the second leading cause of cancer-related death by 2030. Despite intensive research, the five-year overall survival rate remains dismally low at less than 15% (Siegel, Kratzer et al. 2025, Nagaraju, Nellipudi et al. 2026). This exceptionally high mortality is primarily driven by its asymptomatic early progression, extensive local invasion, and an extreme propensity for early systemic dissemination (Leroux and Konstantinidou 2021, Remond, Pellat et al. 2022, Zheng, Liu et al. 2024). Moreover, owing to its complex molecular heterogeneity and highly refractory nature, recent advances in surgical modalities, targeted agents, and immunotherapies have yielded highly limited clinical benefits for the patients (Balachandran, Beatty et al. 2019, Liudahl, Betts et al. 2021, Brautigam, Skok et al. 2025). Consequently, elucidating the core molecular determinants driving PDAC malignant progression and metastasis is urgently required to identify reliable prognostic biomarkers and develop novel, effective targeted interventions.

Tumor metastasis is a highly coordinated and dynamic process that relies heavily on the continuous remodeling of the actin cytoskeleton, which governs cell morphological changes, motility, and invasion (Davidson, Strand et al. 2023, Jagodnik, Dekel et al. 2024). The tropomodulin (TMOD) family consists of

highly conserved actin-binding proteins that stabilize microfilaments by capping their slow-growing (pointed) ends, thereby arresting the association and dissociation of G-actin monomers (Parreno and Fowler 2018). This family comprises four distinct isoforms (TMOD1–4), each characterized by a highly specific, tissue-dependent expression profile (Colpan, Moroz et al. 2013). TMOD3 is a ubiquitous actin-capping protein that strictly regulates actin filament dynamics by binding to the pointed ends of actin filaments (Parreno and Fowler 2018). While TMOD3 has been extensively studied in the context of embryonic development and erythrocyte structural integrity, emerging evidence suggests its dysregulation in several human malignancies (Chen, Wang et al. 2022). For instance, aberrant TMOD3 expression has been linked to enhanced cell migration and tumor growth in hepatocellular carcinoma and bladder cancer (Zheng, Yang et al. 2019, Tian, He et al. 2024). However, the precise expression pattern, clinical significance, and biological function of TMOD3 in the context of pancreatic cancer remain completely elusive.

To exert their biological functions in cancer cells, cytoskeletal regulators often orchestrate complex protein-protein interaction (PPI) networks to trigger downstream signaling cascades. Leucine-rich repeat flightless-interacting protein 1 (LRRFIP1) is a versatile cytosolic protein known to act as an important mediator in cytoskeletal organization, transcriptional regulation, and various intracellular signaling pathways (Takimoto 2019). Recent studies have highlighted the critical role of LRRFIP1 in tumor biology, demonstrating its involvement in promoting the proliferation, invasion, and chemoresistance of certain cancer cells (Kawasaki, Ohtsuka et al. 2021, Li, Tuo et al. 2024). Given the shared involvement of TMOD3 and LRRFIP1 in cytoskeletal dynamics and cellular motility, we hypothesized a functional and physical interplay between these two proteins in driving the malignant phenotypes of PDAC.

In this study, we identify TMOD3 as a potent oncogenic driver and a robust prognostic biomarker in pancreatic cancer. We demonstrate that TMOD3 is significantly upregulated in PDAC tissues and strongly correlates with advanced tumor stages and poor patient overall survival. Through comprehensive *in vitro* and *in vivo* models, we establish that TMOD3 overexpression markedly accelerates PDAC cell proliferation, migration, invasion, and lung metastasis. Mechanistically, we uncover a direct physical interaction between TMOD3 and LRRFIP1. Importantly, we show that the tumor-promoting effects of TMOD3 are fundamentally dependent on LRRFIP1, without altering its transcriptional levels. Our findings elucidate the novel TMOD3/LRRFIP1 axis as a critical vulnerability in pancreatic cancer progression, offering a compelling rationale for targeting this functional complex in future therapeutic interventions.

Materials and Methods

1. Bioinformatics Analysis

The mRNA expression levels of TMOD3 and LRRFIP1 in PDAC and adjacent normal tissues were analyzed using the GEPIA database (http://gepia.cancer-pku.cn/), which integrates data from the TCGA and GTEx projects. Overall survival (OS) analyses of PDAC patients based on TMOD3 and LRRFIP1

expression levels were also performed using the survival plots module in GEPIA. The potential protein-protein interaction (PPI) network of TMOD3 was predicted using the STRING database (https://string-db.org/).

2. Cell Culture

The human (Homo sapiens) pancreatic ductal carcinoma cell line PANC-1 (sex: male; RRID: CVCL_0480) and pancreatic adenocarcinoma cell line BxPC-3 (sex: female; RRID: CVCL_0186) were obtained from the Cell Bank of the Chinese Academy of Sciences (Shanghai, China) in [Insert Month, Year]. Both cell lines were authenticated by the supplier using short tandem repeat (STR) profiling. We confirmed that these cell lines have not been previously reported as misidentified or contaminated according to the International Cell Line Authentication Committee (ICLAC) register. Furthermore, all cell lines were routinely tested and confirmed to be free of mycoplasma contamination prior to and during the described experiments using a PCR-based mycoplasma detection kit (Thermo, Grand Island, NY, USA; Cat# 4460626). PANC-1 cells were cultured in Dulbecco's Modified Eagle Medium (DMEM; Gibco, Grand Island, NY, USA; Cat# 11965092), and BxPC-3 cells were cultured in RPMI-1640 medium (Gibco; Cat# 11875093). Both media were supplemented with 10% fetal bovine serum (FBS; Gibco; Cat# 10099141) and 1% penicillin-streptomycin (10,000 U/mL; Gibco; Cat# 15140122). Cells were maintained in a humidified incubator at 37°C with 5% CO2.

3. Tissue Microarray (TMA) and Immunohistochemistry (IHC)

A human pancreatic cancer tissue microarray containing PDAC tissues and adjacent normal tissues (with patient survival data and clinicopathological characteristics) was purchased from Biotechwell (Cat#ZL-PACSur1602, Shanghai, China). The TMA slides were deparaffinized in xylene, rehydrated through graded ethanols, and subjected to antigen retrieval using citrate buffer (pH 6.0). After blocking endogenous peroxidase activity with 3% H_2O_2, the slides were incubated with a primary antibody against TMOD3 (1:200 dilution; Proteintech, Wuhan, China; Cat# 11495-1-AP) overnight at 4°C. The sections were then incubated with an HRP-conjugated secondary antibody, visualized using a DAB Substrate Kit (Beyotime, Shanghai, China; Cat# P0203), and counterstained with hematoxylin. The IHC staining was independently evaluated and scored by two pathologists based on the staining intensity and the percentage of positive cells.

4. Plasmids, siRNAs, and Cell Transfection

Small interfering RNAs (siRNAs) specifically targeting TMOD3 (siTMOD3-1, -2, -3) and LRRFIP1 (siLRRFIP1), as well as the negative control siRNA (siNC), were designed and synthesized by GenePharma (Shanghai, China). The TMOD3 overexpression plasmid (pcDNA3.1-TMOD3) and the empty vector were purchased from General Biosystems (Anhui, China). Cell transfections were performed using

Lipofectamine 3000 Reagent (Invitrogen, Carlsbad, CA, USA; Cat# L3000015) according to the manufacturer's instructions. For *in vivo* experiments, lentiviruses encoding short hairpin RNAs targeting TMOD3 (shTMOD3) or LRRFIP1 (shLRRFIP1), alongside negative controls (shNC), were synthesized by General Biosystems (Anhui, China). Stably transfected cells were selected using 2 μg/mL puromycin (Sigma-Aldrich, St. Louis, MO, USA; Cat# P8833) for 2 weeks.

5. RNA Extraction and Quantitative Real-Time PCR (RT-qPCR)

Total RNA was extracted from cultured cells using TRIzol Reagent (Invitrogen; Cat# 15596026). RNA was reverse-transcribed into cDNA using the PrimeScript™ RT Reagent Kit (TaKaRa, Kusatsu, Japan; Cat# RR037A). Quantitative real-time PCR was performed using TB Green® Premix Ex Taq™ II (TaKaRa; Cat# RR820A) on an ABI StepOnePlus Real-Time PCR System (Applied Biosystems, Foster City, CA, USA). GAPDH was used as an endogenous control. The relative mRNA expression levels were calculated using the $2^{-\Delta\Delta Ct}$ method.

6. Western Blotting and Co-Immunoprecipitation (Co-IP)

6. Western Blotting and Co-Immunoprecipitation (Co-IP)
For Western blotting, cells were lysed using RIPA buffer (Beyotime; Cat# P0013B) supplemented with a protease inhibitor cocktail (Roche, Basel, Switzerland). Protein concentrations were measured using a BCA Protein Assay Kit (Thermo Fisher Scientific, Waltham, MA, USA; Cat# 23225). Equal amounts of protein were separated by SDS-PAGE and transferred onto PVDF membranes (Millipore, Billerica, MA, USA). After blocking with 5% non-fat milk, the membranes were incubated with primary antibodies against TMOD3 (Proteintech; Cat# 11495-1-AP), LRRFIP1 (Abcam, Cambridge, UK; Cat# ab122329), and GAPDH (Cell Signaling Technology, Danvers, MA, USA; Cat# 5174, 1:1000) overnight at 4°C, followed by incubation with appropriate HRP-conjugated secondary antibodies. Protein bands were visualized using an ECL detection system (Millipore; Cat# WBKLS0500).

For Co-IP assays, pre-cleared cell lysates were incubated with specific anti-TMOD3 or anti-LRRFIP1 antibodies, or normal IgG (as a control) overnight at 4°C. Protein A/G Magnetic Beads (Thermo Fisher Scientific; Cat# 88802) were then added to the lysates and incubated for 2 hours at room temperature. The beads were washed, boiled in SDS loading buffer, and the interacting proteins were analyzed by Western blotting.

7. Cell Viability and EdU Proliferation Assays

Cell viability was assessed using the Cell Counting Kit-8 (CCK-8; Dojindo, Kumamoto, Japan; Cat# CK04). Transfected cells were seeded into 96-well plates at a density of 2,000 cells/well. At designated time points (0, 24, 48, 72, and 96 hours), 10 μL of CCK-8 solution was added to each well and incubated for 2

hours at 37°C. The optical density (OD) at 450 nm was measured using a microplate reader (Bio-Rad, Hercules, CA, USA).

For the EdU assay, cell proliferation was evaluated using the Cell-Light EdU Apollo567 In Vitro Kit (RiboBio, Guangzhou, China; Cat# C10310-1) according to the manufacturer's protocol. The nuclei were counterstained with DAPI, and the proportion of EdU-positive cells was observed and captured under a fluorescence microscope (Olympus, Tokyo, Japan).

8. Wound Healing, Cell Migration, and Invasion Assays

For the wound healing assay, cells were seeded into 6-well plates and cultured to 90% confluence. A linear scratch was made using a sterile 200 µL pipette tip. After washing with PBS, cells were cultured in serum-free medium for 24 hours. Images of the scratches were captured at 0 and 24 hours under a microscope, and the relative migration distance was calculated.

Transwell assays were performed using 8.0-µm pore size Transwell chambers (Corning, NY, USA; Cat# 3422). For the invasion assay, the upper chambers were pre-coated with Matrigel (BD Biosciences, San Jose, CA, USA; Cat# 356234). 5×10^4 cells suspended in 200 µL of serum-free medium were added to the upper chamber, while 600 µL of medium containing 10% FBS was added to the lower chamber as a chemoattractant. After 24–48 hours of incubation, the cells remaining on the upper surface were removed, and the migrated/invaded cells on the lower surface were fixed with 4% paraformaldehyde and stained with 0.1% crystal violet. Cells were counted in five randomly selected fields under a microscope.

9. In Vivo Animal Experiments

All animal procedures were approved by the Animal Ethics Committee of Wuhan Servicebio Technology Co., Ltd. Four-week-old male BALB/c nude mice were purchased from Vital River Laboratory Animal Technology Co., Ltd. (Beijing, China) and housed in specific pathogen-free (SPF) conditions.

For the subcutaneous tumor xenograft model, 5×10^6 stably transfected pancreatic cancer cells were suspended in 100 µL PBS and subcutaneously injected into the right flank of the mice (n = 5 per group). Tumor dimensions were measured every 5 days using digital calipers, and tumor volume was calculated as Volume = (length x width^2)/2. Mice were sacrificed 30 days post-injection, and the tumors were excised, photographed, and weighed.

For the lung metastasis model, 2×10^6 stably transfected cells were injected into the tail veins of nude mice. The mice were sacrificed 6 weeks after injection. The lungs were excised, fixed in 4% paraformaldehyde, embedded in paraffin, sectioned, and subjected to standard Hematoxylin and Eosin (H&E) staining to evaluate metastatic nodules.

10. Statistical Analysis

All quantitative data are presented as the mean ± standard deviation (SD) from at least three independent experiments. Statistical analyses were performed using GraphPad Prism 8.0 software (GraphPad Software, San Diego, CA, USA). Differences between two groups were analyzed using Student's *t*-test, while multi-group comparisons were evaluated by One-way ANOVA. Survival curves were generated using the Kaplan-Meier method and compared using the Log-rank test. The correlation between two variables was assessed using Pearson correlation analysis. A two-sided $p < 0.05$ was considered statistically significant (* $p < 0.05$, $p < 0.01$, *** $p < 0.001$).

Results

TMOD3 is upregulated in pancreatic cancer and correlates with poor prognosis

To investigate the expression pattern and clinical significance of TMOD3 in pancreatic adenocarcinoma (PDAC), we first evaluated the differential expression of TMOD3 between tumor and normal tissues using the GEPIA database. The results revealed that the transcriptional level of TMOD3 was significantly elevated in PDAC tissues (n=179) compared to normal pancreatic tissues (n=171) (**Figure 1A**). Subsequent overall survival (OS) analysis demonstrated that patients with high TMOD3 expression (n=89) exhibited a significantly shorter OS than those with low TMOD3 expression (n=89) (Log-rank $p = 0.00024$, **Figure 1B**), indicating a potential tumor-promoting role of TMOD3 in PDAC progression.

To validate these findings at the protein level, we performed immunohistochemistry (IHC) staining on a tissue microarray (TMA) containing pancreatic cancer tissues and adjacent normal tissues. Representative images showed that the protein expression of TMOD3 was markedly upregulated in pancreatic cancer tissues compared with normal tissues (**Figure 1C**). Based on the IHC scores, the TMA cohort of 79 patients was divided into a TMOD3-high group (n=24) and a TMOD3-low group (n=55). Kaplan-Meier survival analysis further confirmed that elevated TMOD3 expression was significantly associated with reduced overall survival in pancreatic cancer patients ($p < 0.0001$, **Figure 1D**). Moreover, we analyzed the correlation between TMOD3 expression and clinicopathological characteristics in this TMA cohort (**Table 1**). Chi-square test results indicated that aberrant TMOD3 overexpression was significantly correlated with advanced T stage ($p < 0.001$) and survival status ($p = 0.0001$), whereas no significant associations were observed with gender, tumor location, perineural invasion, vascular invasion, lymph node metastasis, distant metastasis, AJCC stage group, or histological grade. Taken together, these results demonstrate that TMOD3 is significantly highly expressed in pancreatic cancer and may serve as a potential prognostic biomarker for PDAC patients.

Knockdown of TMOD3 inhibits the proliferation, migration, and invasion of pancreatic cancer cells *in vitro*

To further investigate the biological function of TMOD3 in pancreatic cancer, we performed loss-of-function assays in two pancreatic cancer cell lines, PANC-1 and BxPC3. First, we designed three specific

small interfering RNAs (siTMOD3-1, -2, and -3) targeting TMOD3 and evaluated their knockdown efficiencies. RT-qPCR results revealed that all three siRNAs significantly decreased the mRNA levels of TMOD3 in both PANC-1 and BxPC3 cells compared to the negative control (siNC) (**Figure S1A**). We selected siTMOD3-1 and siTMOD3-2, which exhibited the highest silencing efficiencies, for subsequent experiments. Western blot analysis further confirmed that both selected siRNAs robustly reduced the protein expression of TMOD3 in these two cell lines (**Figure S1B**).

Following the successful knockdown of TMOD3, cell viability assays demonstrated that silencing TMOD3 significantly attenuated the growth rate of both PANC-1 and BxPC3 cells compared to the siNC group (**Figure 2A**). Consistently, EdU incorporation assays revealed a marked reduction in the percentage of actively proliferating (EdU-positive) cells following TMOD3 depletion (**Figure 2B**). Furthermore, we assessed the effect of TMOD3 on the metastatic potential of pancreatic cancer cells. Transwell assays with or without Matrigel coating indicated that the depletion of TMOD3 drastically impaired both the migratory and invasive capacities of PANC-1 and BxPC3 cells (**Figure 2C**). In addition, wound healing assays showed that the rate of scratch closure was significantly delayed in the TMOD3 knockdown groups compared with the control cells (**Figure 2D**). Collectively, these *in vitro* findings indicate that TMOD3 serves as an oncogene that promotes the proliferation, migration, and invasion of pancreatic cancer cells.

Knockdown of TMOD3 suppresses pancreatic cancer growth and metastasis *in vivo*

To further validate the oncogenic role of TMOD3 *in vivo*, we established a subcutaneous xenograft tumor model by injecting pancreatic cancer cells stably expressing short hairpin RNA against TMOD3 (shTMOD3) or negative control shRNA (shNC) into nude mice. Consistent with our *in vitro* findings, tumors derived from the shTMOD3 group were visibly smaller than those from the shNC group (**Figure 3A**). The tumor volume growth curve over a 30-day period demonstrated that silencing TMOD3 significantly decelerated tumor growth compared to the control group (**Figure 3B**). At the endpoint of the experiment, the excised tumors were weighed, revealing a significant reduction in tumor weight in the TMOD3-knockdown group (**Figure 3C**). These results indicate that TMOD3 depletion profoundly inhibits the tumorigenicity and growth of pancreatic cancer *in vivo*.

Furthermore, we utilized a tail vein injection model to evaluate the effect of TMOD3 on the metastatic capacity of pancreatic cancer cells *in vivo*. Histological examination of lung tissues using Hematoxylin and Eosin (H&E) staining revealed that mice injected with shTMOD3 cells developed fewer and smaller lung metastatic nodules compared to the control group. Quantitative analysis further confirmed that the percentage of lung area occupied by metastatic lesions was significantly decreased following TMOD3 knockdown (**Figure 3D**). Collectively, these *in vivo* data strongly support the conclusion that TMOD3 promotes both the progression and metastasis of pancreatic cancer.

TMOD3 physically interacts with LRRFIP1 in pancreatic cancer cells

To explore the molecular mechanisms underlying TMOD3-driven malignant progression in pancreatic cancer, we performed a predictive analysis of potential TMOD3-interacting proteins using the STRING database. The protein-protein interaction (PPI) network revealed that TMOD3 potentially interacts with multiple proteins, including LRRFIP1 (**Figure 4A**). Given the established role of LRRFIP1 in cytoskeleton remodeling, cell migration, and tumor-associated signal transduction, as well as its involvement in malignant biological processes such as proliferation and invasion, we hypothesized that LRRFIP1 might serve as a crucial downstream effector mediating TMOD3-induced pancreatic cancer progression.

To support this hypothesis, we first analyzed the correlation between TMOD3 and LRRFIP1 expression using the GEPIA dataset. The results demonstrated a significant positive correlation between the mRNA expression levels of TMOD3 and LRRFIP1 in pancreatic cancer tissues (R = 0.54, p = 3.6e-15; **Figure 4B**). To experimentally validate this interaction, we performed endogenous co-immunoprecipitation (Co-IP) assays in two pancreatic cancer cell lines. The reciprocal Co-IP results clearly showed that TMOD3 and LRRFIP1 physically interact with each other in both PANC-1 (**Figure 4C**) and BxPC3 (**Figure 4D**) cells. To further elucidate the regulatory relationship between TMOD3 and LRRFIP1, we examined whether TMOD3 modulates LRRFIP1 at the transcriptional level. Interestingly, RT-qPCR analysis demonstrated that neither the overexpression (**Figure S2A**) nor the knockdown (**Figure S2B**) of TMOD3 significantly altered the mRNA levels of LRRFIP1 in PANC-1 and BxPC3 cells. These findings indicate that TMOD3 does not regulate LRRFIP1 transcriptionally, but rather interacts with it directly at the protein level.

Furthermore, we evaluated the expression and clinical relevance of LRRFIP1 in pancreatic cancer using the GEPIA database. Similar to TMOD3, LRRFIP1 was found to be significantly upregulated in pancreatic cancer tissues (n=179) compared to normal pancreatic tissues (n=171) (**Figure 4E**). Survival analysis indicated that patients with high LRRFIP1 expression tended to have a worse overall survival, although the difference did not reach strict statistical significance in this specific dataset (Log-rank p = 0.13; **Figure 4F**). Taken together, these data indicate that TMOD3 physically binds to LRRFIP1 and is positively correlated with its expression in pancreatic cancer.

LRRFIP1 is essential for TMOD3-mediated proliferation, migration, and invasion in pancreatic cancer cells

To determine whether LRRFIP1 serves as a functional downstream effector mediating the oncogenic role of TMOD3, we performed rescue experiments. PANC-1 and BxPC3 cells were co-transfected with a TMOD3 overexpression plasmid (or empty vector) and LRRFIP1-specific siRNA (siLRRFIP1) or negative control siRNA (siNC).

Cell viability assays (CCK-8) demonstrated that the overexpression of TMOD3 significantly enhanced the proliferative capacity of both PANC-1 and BxPC3 cells compared to the control group. However, this pro-proliferative effect induced by TMOD3 was dramatically abrogated by the concurrent knockdown of LRRFIP1 (**Figure 5A**). Furthermore, Transwell migration and invasion assays revealed that the profound increases in cell migratory and invasive abilities driven by TMOD3 overexpression were significantly reversed upon LRRFIP1 silencing in both pancreatic cancer cell lines (**Figure 5B**). Collectively, these

findings indicate that LRRFIP1 is functionally required for TMOD3-induced malignant phenotypes, and that TMOD3 promotes the aggressive progression of pancreatic cancer in an LRRFIP1-dependent manner.

LRRFIP1 knockdown abrogates TMOD3-promoted pancreatic cancer growth *in vivo*

To further substantiate whether TMOD3 exerts its oncogenic functions through LRRFIP1 *in vivo*, we established a subcutaneous xenograft mouse model. Nude mice were injected with pancreatic cancer cells stably transfected with an empty vector (Vector), a TMOD3 overexpression construct (TMOD3), or a combination of TMOD3 overexpression and shRNA targeting LRRFIP1 (TMOD3+shLRRFIP1).

Consistent with our *in vitro* findings, the *in vivo* results demonstrated that the overexpression of TMOD3 significantly accelerated tumor growth, resulting in markedly larger tumors compared to the control Vector group (**Figure 6A**). However, the concurrent silencing of LRRFIP1 drastically reversed the tumor-promoting effect induced by TMOD3. The tumor growth curve over a 30-day period showed that tumors in the TMOD3+shLRRFIP1 group grew at a significantly slower rate than those in the TMOD3 overexpression group, dropping back to levels comparable to or even lower than the baseline control (**Figure 6B**). Furthermore, quantitative analysis of the excised xenografts at the endpoint revealed that the profound increase in tumor weight driven by TMOD3 was completely abolished upon LRRFIP1 depletion (**Figure 6C**). Taken together, these *in vivo* data compellingly demonstrate that TMOD3 drives the tumorigenicity and aggressive growth of pancreatic cancer in an LRRFIP1-dependent manner.

Discussion

Pancreatic ductal adenocarcinoma remains one of the most formidable challenges in modern oncology, characterized by profound therapeutic resistance and an exceptionally high mortality rate (Mannucci and Goel 2026, Qi, Lv et al. 2026, Salgado-Pascual, Zalba et al. 2026). As current standard-of-care regimens offer strictly limited clinical benefit, there is an immediate and critical need to develop novel, effective therapeutic interventions. In the present study, we unveil a previously unrecognized oncogenic axis orchestrated by TMOD3 and LRRFIP1. Rather than merely cataloging another overexpressed gene in cancer, our findings elucidate a profound functional dependency between these two cytoskeletal regulators, establishing the TMOD3/LRRFIP1 protein complex as a fundamental driver of PDAC progression.

The dynamic remodeling of the actin cytoskeleton is a prerequisite for the acquisition of invasive phenotypes in carcinoma cells (Park, Burckhardt et al. 2020, Tuntithavornwat, Shea et al. 2022, Davidson, Strand et al. 2023). While TMOD3 has been canonically characterized as an actin-capping protein essential for erythrocyte membrane stability (Sui, Nowak et al. 2014), emerging sporadic evidence has hinted at its involvement in solid tumors (Chen, Wang et al. 2022, He, Zheng et al. 2025, Liu, Wang et al. 2025). Our study systematically establishes TMOD3 as a robust prognostic biomarker and a bona fide oncogene in pancreatic cancer. The pronounced attenuation of cellular proliferation, migration, and *in vivo* lung metastasis upon TMOD3 depletion underscores its indispensable role in navigating the

metastatic cascade. Crucially, the clinical correlation between elevated TMOD3 expression and poor overall survival in our TMA cohort reinforces its potential utility in clinical risk stratification for PDAC patients.

A central conundrum in cytoskeletal oncology is how structural proteins translate biomechanical changes into sustained malignant behaviors (Jagodnik, Dekel et al. 2024, Yang, Qin et al. 2024). Our mechanistic investigations provide a compelling answer by identifying LRRFIP1 as the critical effector of TMOD3. LRRFIP1 is a multi-functional protein implicated not only in cytoskeletal organization but also in the transduction of oncogenic signals (Kawasaki, Ohtsuka et al. 2021, Li, Tuo et al. 2024). Interestingly, our data revealed a robust physical interaction between TMOD3 and LRRFIP1, yet alterations in TMOD3 levels did not affect the transcriptional expression of LRRFIP1. This non-transcriptional regulatory mode strongly implies that TMOD3 may function as a structural scaffold or a stabilizing chaperone for LRRFIP1. We speculate that TMOD3 might recruit LRRFIP1 to specific subcellular domains-such as the leading edge of migrating cells or invadopodia-thereby spatially amplifying downstream invasion-related signaling (Shoib, Lodi et al. 2022, Davidson, Strand et al. 2023). The fact that silencing LRRFIP1 almost completely abolished the TMOD3-driven malignant phenotypes *in vitro* and *in vivo* explicitly demonstrates that TMOD3 hijacks the functions of LRRFIP1 to confer an aggressive advantage to pancreatic cancer cells.

From a therapeutic perspective, the identification of the TMOD3/LRRFIP1 interaction opens novel avenues for intervention. While directly targeting the ubiquitous actin cytoskeleton is notoriously toxic due to severe off-target effects on normal cells, disrupting specific tumor-promoting protein-protein interactions (PPIs) represents a more precise strategy. The structural interface between TMOD3 and LRRFIP1 could potentially serve as a druggable vulnerability. The development of specific peptide inhibitors or small-molecule degraders (e.g., PROTACs) designed to uncouple the TMOD3/LRRFIP1 complex might offer a precise therapeutic window to halt pancreatic cancer metastasis without globally paralyzing normal cellular motility. Despite these promising findings, several limitations in our study warrant further investigation. First, the precise molecular interface and the specific binding domains mediating the TMOD3-LRRFIP1 interaction remain to be mapped via crystallographic or truncation analyses. Second, while we established the functional necessity of LRRFIP1 downstream of TMOD3, the exact signaling cascades (e.g., kinases or transcription factors) subsequently hyperactivated by this complex in PDAC require deeper multi-omic profiling. Finally, as our *in vivo* models primarily utilized immunodeficient mice, the potential immunomodulatory effects of the TMOD3/LRRFIP1 axis within the complex tumor microenvironment (TME) of pancreatic cancer remain an open question for future studies.

In conclusion, our work deciphers a novel mechanistic paradigm in pancreatic cancer progression. We demonstrate that TMOD3 operates far beyond a simple cytoskeletal building block; it actively drives tumor proliferation and metastasis by structurally assembling with LRRFIP1. This TMOD3/LRRFIP1 signaling node not only refines our understanding of metastasis biology but also highlights a promising

prognostic indicator and a viable therapeutic target for the clinical management of pancreatic adenocarcinoma.

Abbreviations

PDAC, Pancreatic ductal adenocarcinoma

TMOD3, Tropomodulin 3

TMA, tissue microarray

DMEM, Dulbecco's Modified Eagle Medium

shRNAs, Short hairpin RNAs

CCK-8, Cell Counting Kit-8

LRRFIP1, Leucine-rich repeat flightless-interacting protein 1

Co-IP: Co-immunoprecipitation

IHC: Immunohistochemistry

RT-qPCR: Quantitative Real-Time PCR

Declarations

Availability of Data and Materials

The datasets used or analyzed during the current study are available from the corresponding author on reasonable request.

Author Contributions

CS and XYQ performed the research and collected experimental data. LC and JT provided technical assistance for experiments, performed the research and sample processing, and analyzed the data using statistical methods. CS and XYQ analyzed the data using statistical methods. LX designed the study, supervised the research process and provided essential conceptual advice. CS and LX wrote the first draft of the manuscript. All authors contributed to critical revision of the manuscript for important

intellectual content. All authors read and approved the final manuscript. All authors have participated sufficiently in the work and agreed to be accountable for all aspects of the work.

Funding

This study was supported by the Science and Technology Planning Project of Jiaxing City (2023AD31063), and the Construction Project of National Key Clinical Specialty-Department of Oncology (2023-GJZK-001).

Acknowledgment

Not applicable.

Conflict of Interest

The authors declare no conflict of interest.

Ethics Approval and Consent to Participate

Animal experiments were approved by the Institutional Animal Care and Use Committee of the Institutional Ethics Committee of Wuhan Servicebio Technology Co., Ltd.

References

1. Balachandran, V. P., G. L. Beatty and S. K. Dougan (2019). "Broadening the Impact of Immunotherapy to Pancreatic Cancer: Challenges and Opportunities." Gastroenterology **156**(7): 2056-2072.
2. Brautigam, K., K. Skok, K. Szymonski, C. V. Rift and E. Karamitopoulou (2025). "Tumor immune microenvironment in pancreatic ductal adenocarcinoma revisited - Exploring the "Space"." Cancer Lett **622**: 217699.
3. Chen, B., M. Wang, J. Qiu, K. Liao, W. Zhang, Q. Lv, C. Ma, Z. Qian, Z. Shi, R. Liang, Y. Lin, J. Ye, Y. Qiu and Y. Lin (2022). "Cleavage of tropomodulin-3 by asparagine endopeptidase promotes cancer malignancy by actin remodeling and SND1/RhoA signaling." J Exp Clin Cancer Res **41**(1): 209.
4. Colpan, M., N. A. Moroz and A. S. Kostyukova (2013). "Tropomodulins and tropomyosins: working as a team." J Muscle Res Cell Motil **34**(3-4): 247-260.
5. Davidson, J., M. Strand, D. Cullinan, M. Scherer, A. Zafar, J. Martinie, D. Vrochides, W. Chapman, M. Doyle and A. Khan (2023). "The importance of robotic surgery training in HPB fellowship: a survey of the 2022 AHPBA fellows." HPB (Oxford) **25**(10): 1203-1212.
6. He, Z., D. Zheng, F. Li, L. Chen, C. Wu, Z. Zeng and C. Yu (2025). "TMOD3 accelerated resistance to immunotherapy in KRAS-mutated pancreatic cancer through promoting autophagy-dependent degradation of ASCL4." Drug Resist Updat **78**: 101171.

7. Jagodnik, K. M., S. Dekel and A. Bartal (2024). "Persistence of collective memory of corporate bankruptcy events discussed on X (Twitter) is influenced by pre-bankruptcy public attention." Sci Rep **14**(1): 6552.
8. Kawasaki, S., H. Ohtsuka, Y. Sato, D. Douchi, M. Sato, K. Ariake, K. Masuda, K. Fukase, M. Mizuma, K. Nakagawa, H. Hayashi, T. Morikawa, F. Motoi and M. Unno (2021). "Silencing of LRRFIP1 enhances the sensitivity of gemcitabine in pancreatic cancer cells by activating JNK/c-Jun signaling." Pancreatology **21**(4): 771-778.
9. Leroux, C. and G. Konstantinidou (2021). "Targeted Therapies for Pancreatic Cancer: Overview of Current Treatments and New Opportunities for Personalized Oncology." Cancers (Basel) **13**(4).
10. Li, J., D. Tuo, G. Guo, Y. Gao and J. Gan (2024). "The clinical significance and oncogenic function of LRRFIP1 in pancreatic cancer." Discov Oncol **15**(1): 123.
11. Liu, Y., H. Wang, J. Zhan, J. Sun, Y. Sun, X. Fu, D. Lv, X. Li, T. Dong and H. Lou (2025). "Interaction between CDC6 and Tmod3 accelerates resistance to paclitaxel through focal adhesion assembly." Signal Transduct Target Ther **10**(1): 395.
12. Liudahl, S. M., C. B. Betts, S. Sivagnanam, V. Morales-Oyarvide, A. da Silva, C. Yuan, S. Hwang, A. Grossblatt-Wait, K. R. Leis, W. Larson, M. B. Lavoie, P. Robinson, A. Dias Costa, S. A. Vayrynen, T. E. Clancy, D. A. Rubinson, J. Link, D. Keith, W. Horton, M. A. Tempero, R. H. Vonderheide, E. M. Jaffee, B. Sheppard, J. Goecks, R. C. Sears, B. S. Park, M. Mori, J. A. Nowak, B. M. Wolpin and L. M. Coussens (2021). "Leukocyte Heterogeneity in Pancreatic Ductal Adenocarcinoma: Phenotypic and Spatial Features Associated with Clinical Outcome." Cancer Discov **11**(8): 2014-2031.
13. Mannucci, A. and A. Goel (2026). "Advances in pancreatic cancer early diagnosis, prevention, and treatment: The past, the present, and the future." CA Cancer J Clin **76**(1): e70035.
14. Nagaraju, G. P., H. Nellipudi, C. Ganji, V. Kuppala, S. P. Ganji, S. Kumari, B. Farran, M. Srilatha, R. Guenter and B. F. El-Rayes (2026). "Pancreatic ductal adenocarcinoma: integrating molecular insights for targeted interventions." Signal Transduct Target Ther **11**(1).
15. Park, J. S., C. J. Burckhardt, R. Lazcano, L. M. Solis, T. Isogai, L. Li, C. S. Chen, B. Gao, J. D. Minna, R. Bachoo, R. J. DeBerardinis and G. Danuser (2020). "Mechanical regulation of glycolysis via cytoskeleton architecture." Nature **578**(7796): 621-626.
16. Parreno, J. and V. M. Fowler (2018). "Multifunctional roles of tropomodulin-3 in regulating actin dynamics." Biophys Rev **10**(6): 1605-1615.
17. Qi, H., G. Lv, S. Zhang, R. Xue and M. Liu (2026). "Unraveling pancreatic ductal adenocarcinoma at single-cell resolution with spatial insights: From mechanisms to clinical translation." Cancer Lett **645**: 218391.
18. Remond, M. S., A. Pellat, C. Brezault, M. Dhooge and R. Coriat (2022). "Are targeted therapies or immunotherapies effective in metastatic pancreatic adenocarcinoma?" ESMO Open **7**(6): 100638.
19. Salgado-Pascual, A., S. Zalba, J. J. Lasarte and M. J. Garrido (2026). "Emerging nanoparticle-based therapies for pancreatic cancer: Current clinical landscape." Adv Drug Deliv Rev **229**: 115760.

20. Shoib, S., A. Lodi, A. Saleem, A. Y. Armiya'u, S. Turan and S. Philip (2022). "Public health literacy unsold during panic buying." Ann Med Surg (Lond) **80**: 104156.
21. Siegel, R. L., T. B. Kratzer, A. N. Giaquinto, H. Sung and A. Jemal (2025). "Cancer statistics, 2025." CA Cancer J Clin **75**(1): 10-45.
22. Sui, Z., R. B. Nowak, A. Bacconi, N. E. Kim, H. Liu, J. Li, A. Wickrema, X. L. An and V. M. Fowler (2014). "Tropomodulin3-null mice are embryonic lethal with anemia due to impaired erythroid terminal differentiation in the fetal liver." Blood **123**(5): 758-767.
23. Takimoto, M. (2019). "Multidisciplinary Roles of LRRFIP1/GCF2 in Human Biological Systems and Diseases." Cells **8**(2).
24. Tian, T., S. He, H. Hao, B. Guan, Y. Gong, J. Fan, Z. Zhu, W. Gao, Y. Wu, N. Feng, A. Wang, Y. Guo and X. Li (2024). "YWHAG promotes bladder cancer metastasis by regulating TMOD3 to activate ERK1/2 and JNK phosphorylation in the MAPK pathway." J Transl Med **22**(1): 1159.
25. Tuntithavornwat, S., D. J. Shea, B. S. Wong, T. Guardia, S. J. Lee, C. L. Yankaskas, L. Zheng, A. Kontrogianni-Konstantopoulos and K. Konstantopoulos (2022). "Giant obscurin regulates migration and metastasis via RhoA-dependent cytoskeletal remodeling in pancreatic cancer." Cancer Lett **526**: 155-167.
26. Yang, J., L. Qin, S. Zhou, J. Li, Y. Tu, M. Mo, X. Liu, J. Huang, X. Qin, A. Jiao, W. Wei and P. Yang (2024). "Network pharmacology, molecular docking and experimental study of CEP in nasopharyngeal carcinoma." J Ethnopharmacol **323**: 117667.
27. Zheng, H., Y. Yang, Y. G. Hong, M. C. Wang, S. X. Yuan, Z. G. Wang, F. R. Bi, L. Q. Hao, H. L. Yan and W. P. Zhou (2019). "Tropomodulin 3 modulates EGFR-PI3K-AKT signaling to drive hepatocellular carcinoma metastasis." Mol Carcinog **58**(10): 1897-1907.
28. Zheng, R., X. Liu, Y. Zhang, Y. Liu, Y. Wang, S. Guo, X. Jin, J. Zhang, Y. Guan and Y. Liu (2024). "Frontiers and future of immunotherapy for pancreatic cancer: from molecular mechanisms to clinical application." Front Immunol **15**: 1383978.

Table

Table 1 is available in the Supplementary Files section.

Figures

Figure 2

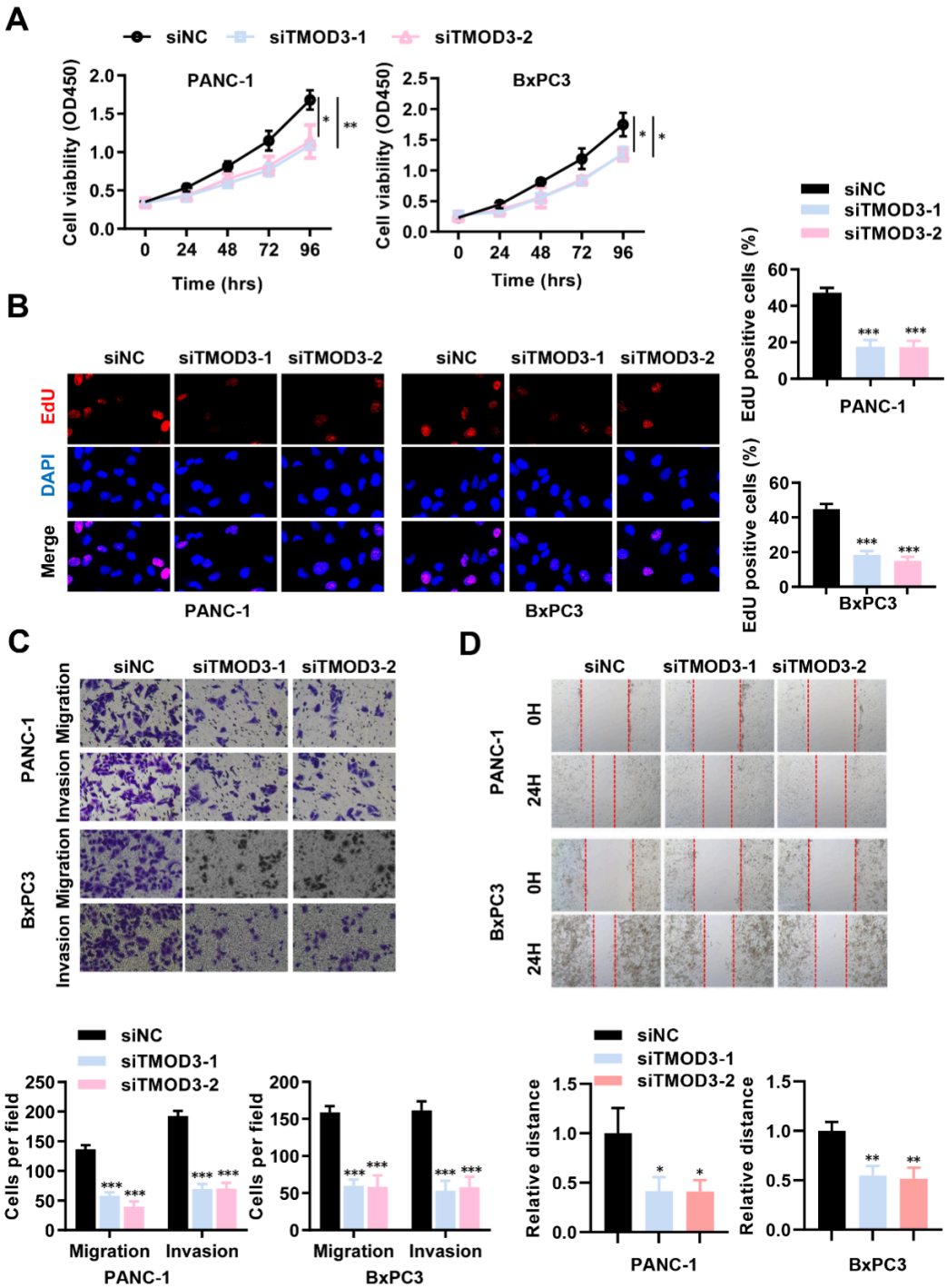


Figure 2

Knockdown of TMOD3 inhibits the proliferation, migration, and invasion of pancreatic cancer cells. (A) The cell viability of PANC-1 and BxPC3 cells transfected with siNC, siTMOD3-1, or siTMOD3-2 was measured at 0, 24, 48, 72, and 96 hours. The optical density (OD450) was recorded to assess cell proliferation (*p < 0.05, p < 0.01). **(B)** EdU assays were performed to evaluate the DNA synthesis and proliferation of PANC-1 and BxPC3 cells after TMOD3 knockdown. Representative images of EdU

staining (red) and DAPI for nuclei (blue) are shown on the left, and the quantification of EdU-positive cells is shown on the right (***p < 0.001). **(C)** Transwell migration and invasion assays of PANC-1 and BxPC3 cells following transfection with the indicated siRNAs. Representative images (top) and the quantitative analysis of migrated/invaded cells per field (bottom) are presented (***p < 0.001). **(D)** Wound healing assays were conducted to assess the migratory ability of PANC-1 and BxPC3 cells upon TMOD3 silencing. Representative images at 0 and 24 hours (top) and the quantitative analysis of the relative migration distance (bottom) are shown (*p < 0.05, p < 0.01). *All data are presented as the mean ± SD from three independent experiments.*

Figure 4

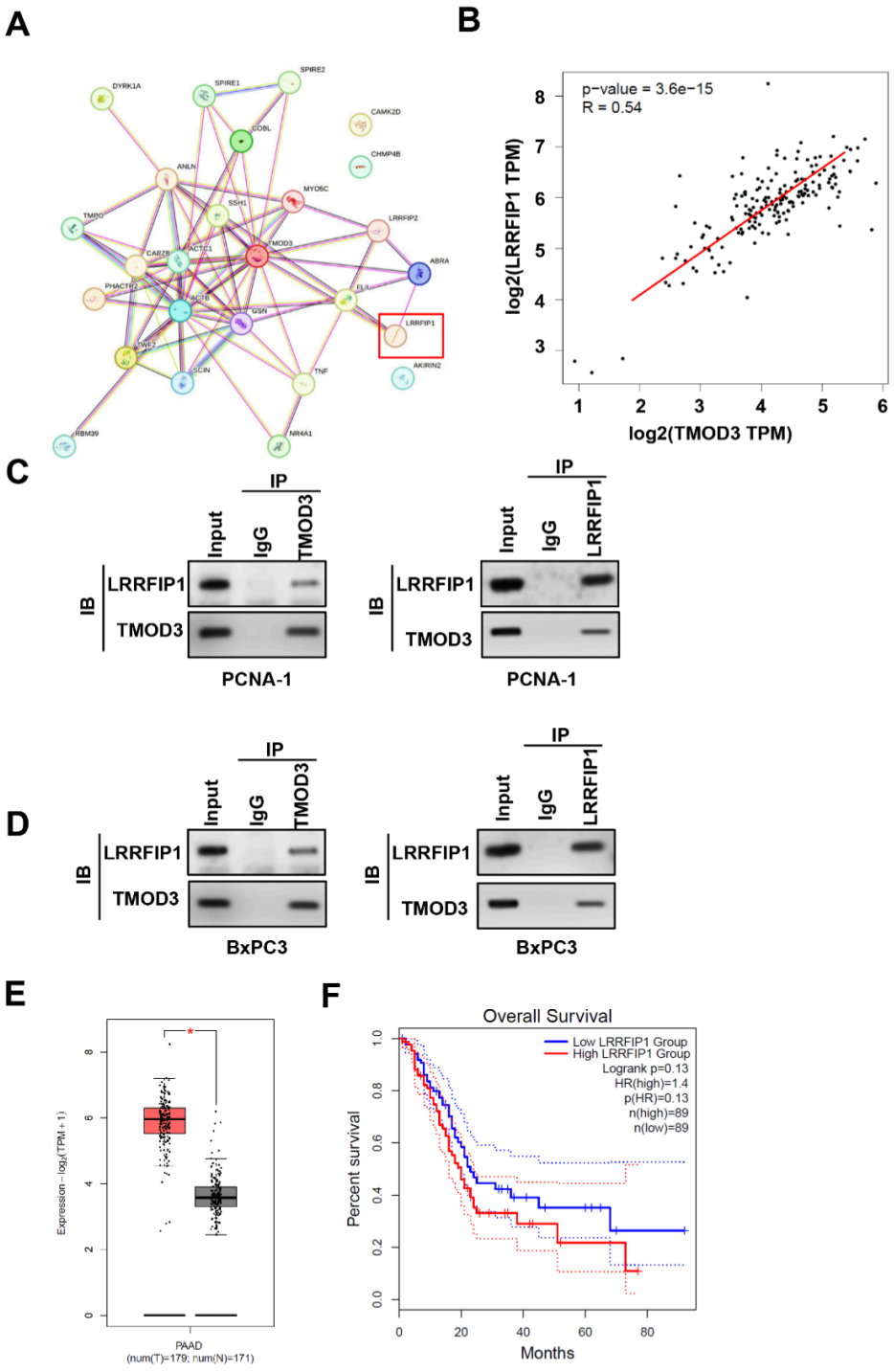


Figure 4

TMOD3 physically interacts with LRRFIP1 and positively correlates with its expression in pancreatic cancer. (A) Protein-protein interaction (PPI) network of TMOD3 predicted by the STRING database. The red box highlights LRRFIP1 as a potential interacting partner. **(B)** Pearson correlation analysis of the mRNA expression levels between TMOD3 and LRRFIP1 in pancreatic adenocarcinoma based on the GEPIA database (R = 0.54, *p* = 3.6e-15). **(C-D)** Endogenous co-immunoprecipitation (Co-IP) assays

demonstrating the physical interaction between TMOD3 and LRRFIP1 in PANC-1 **(C)** and BxPC3 **(D)** cells. Cell lysates were immunoprecipitated (IP) with specific anti-TMOD3 or anti-LRRFIP1 antibodies, followed by immunoblotting (IB) with the indicated antibodies. Normal IgG served as a negative control. **(E)** Box plots showing the mRNA expression levels of LRRFIP1 in pancreatic cancer tissues (PDAC, n=179) and adjacent normal tissues (n=171) from the GEPIA database (*p < 0.05). **(F)**Kaplan-Meier overall survival curve of PDAC patients stratified by LRRFIP1 expression levels (High, n=89; Low, n=89; Logrank *p* = 0.13).

Figure 5

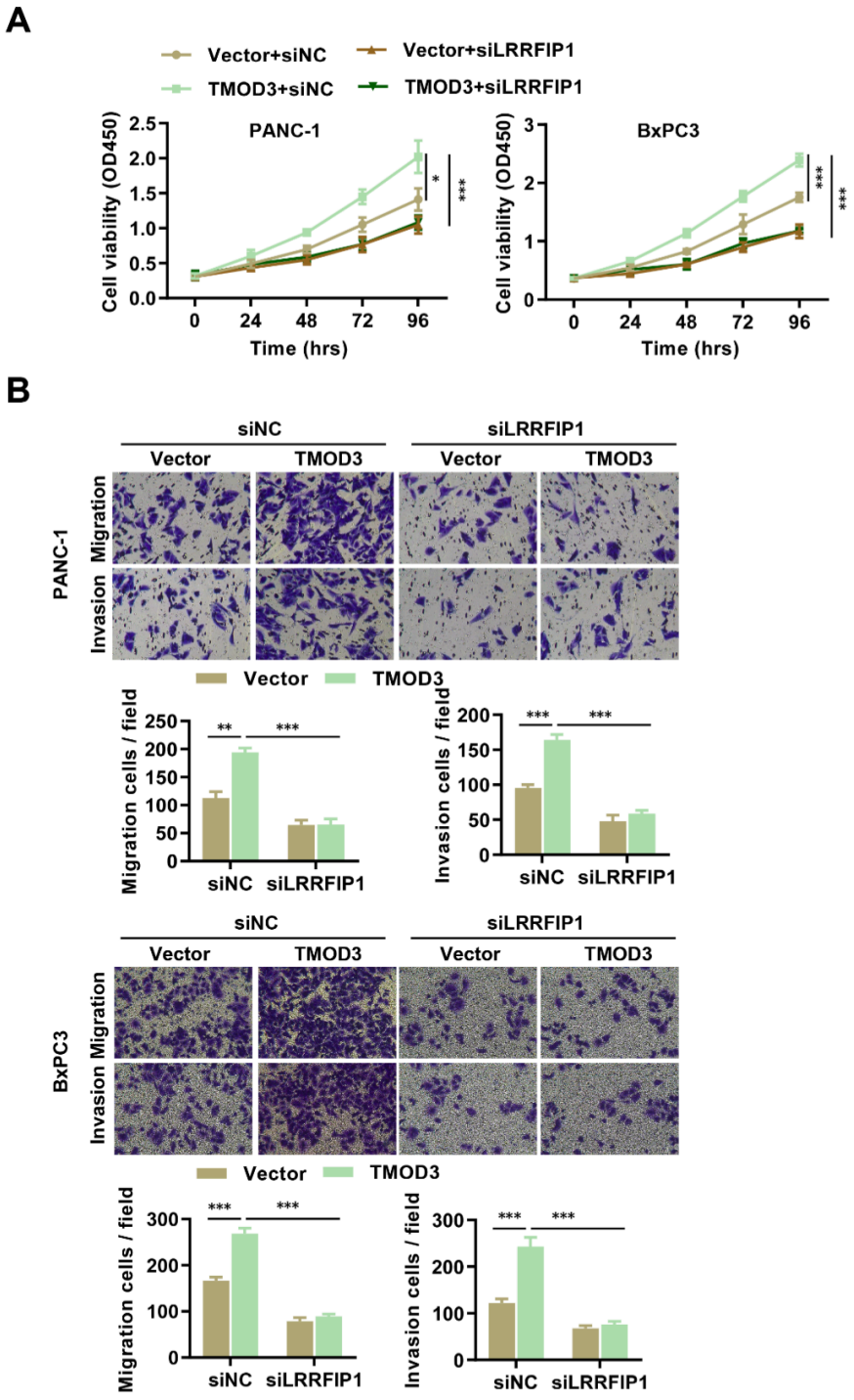


Figure 5

Knockdown of LRRFIP1 abrogates TMOD3-induced proliferation, migration, and invasion in pancreatic cancer cells. (A) Cell viability of PANC-1 and BxPC3 cells co-transfected with the indicated plasmids (Vector or TMOD3) and siRNAs (siNC or siLRRFIP1) was measured by CCK-8 assays at 0, 24, 48, 72, and 96 hours (*p < 0.05, ***p < 0.001). **(B)** Transwell assays assessing the migration and invasion capacities of PANC-1 (top) and BxPC3 (bottom) cells following the indicated co-transfections. Representative images of migrated and invaded cells are shown. The bar graphs represent the quantitative analysis of the number of migrated and invaded cells per field (p < 0.01, ***p < 0.001). All quantitative data are presented as the mean ± SD from three independent experiments.

Supplementary Files

This is a list of supplementary files associated with this preprint. Click to download.

- Supplementaryfigure.pdf
- Table1.docx